GlaucoNet: A Highly Robust Stacked Auto-Encoder assisted Deep Learning Model for Glaucoma Detection System

NaganagoudaPatil, P V Rao

Abstract- ***High pace rise in Glaucoma, an irreversible eye disease that deteriorates vision capacity of human has alarmed academia-industries to develop a novel and robust Computer Aided Diagnosis (CAD) system for early Glaucomatic eye detection. The main root cause for glaucoma growth depends on its structural alterations in the retina and is very much essential for ophthalmologists to identify it at an initial period to stop its progression. Fundoscopy is among one of the biomedical imaging techniques to analyze the internal structure of retina. Recently, numerous efforts have been made to exploit Spatial-Temporal features including morphological values of Optical Disk (OD), Optical Cup (OC), Neuro-Retinal Rim (NRR) etc to perform Glaucoma detection in fundus images. Here, some issues like: suitable pre-processing, precise Region of Interest segmentation, post-segmentation and lack of generalized threshold limits efficacy of the major existing approaches. Furthermore, the optimal segmentation of OD and OC, nerves removal from OD or OC is often tedious and demands more efficient solution. However, these approaches cumulatively turn out to be computationally complex and time-consuming. As potential alternative, deep learning techniques have gained wide-spread attention, especially for image analysis or vision technologies. With this motive, in this paper, the authors proposed a novel Convolutional Stacked Auto-Encoder (CSAE) assisted Deep Learning Model for Glaucoma Detection and Classification model named GlaucoNet. Unlike classical methods, GlaucoNet applies Stacked Auto-Encoder by using hierarchical CNN structure to perform deep feature extraction and learning. By adapting complex data nature, and large features, GlaucoNet was designed with three layers: convolutional layer (CONV), Max-pool layer (MP) and two Fully Connected (FC) layers where the first performs feature extraction and learning, while second exhibits feature selection followed by the reduction of spatial resolution of the individual feature map to avoid large number of parameters and computational complexities. To avoid saturation problem in this work, by marking an applied dropout as 0.5. MATLAB based simulation-results with DRISHTI-GS and DRION-DB datasets affirmed that the proposed GlaucoNet model outperforms as compared to other state-of-art techniques: neural network based approaches in terms of accuracy, recall, precision, F-Measure and balanced accuracy. The overall parametric measured values shown better performance for GlaucoNet model.***

Keywords: Glaucoma detection, Stacked Auto-Encoders, Deep Learning, Convolutional Stacked Auto-Encoder, Computer Aided Diagnosis.

I. INTRODUCTION

The exponential rise in technologies has broadened the horizon for different applications or systems to make human life more efficient, productive and quick decisive. Amongst the major innovations, healthcare sector is the one demanding more attention to make diagnosis more efficient and precise. In the last few years, Computer Aided Diagnosis (CAD) systems have gained worldwide attention across academia-industries to develop more efficient solution; however increase in complexities, symptoms variations, and other key factors such as localized disease traits, different demography etc confine efficiency of the major existing solutions. Considering an example, Glaucoma, which is a type of irreversible eye-disorder or disease, has emerged as one of the most dangerous eye disorder globally that damages optic nerve and degrades vision capacity. However, its growth patterns, size and shape has always been different for different locations or people. In other words, the morphological traits of Optical Cup (OC) and Optical Disc (OD) of a Chinese used to be different than the one from Algeria or Africa. In such case developing a universally applicable model becomes must for accurate or precise Glaucoma detection. Recent study revealed that Glaucoma is the most causative factor for blindness that might reach up to 20 million patients by or before 2020 [1]. In majority, Glaucoma often remains undetected for long time that makes it imperceptible across the early stages. Consequently, we term it as the “silent theft of sight”. In major cases of Glaucoma, a person doesn’t feel any pain or similar symptoms and therefore it can be detected only when it reaches to the advanced stage with more severe symptoms. As already stated, Glaucoma being an irreversible eye-damage disease affects the optical nerve responsible for accommodating information from the eye to the brain and causes blindness and ocular hypertension [2]. Unlike other eye diseases like Myopia or Cataracts, Glaucoma disrupts visio capacity completely and therefore there is the inevitable need to develop a robust CAD solution for precise and early Glaucoma detection and classification (for severity assessment).

Typically, there are three dominant methods for Glaucoma detection; Intraocular Pressure (IOP) measurement, Function-Based Visual Field Test (FBVFT), and Optic Nerve Head (ONH) [4]. Though, IOP signifies a significant risk factor; it can’t be universally robust to detect Glaucoma for different stages with varied clinical-measurement values [3]. On the other hand, FBVFT demands very specific perimetric and sophisticated tools which are costly and

Revised Manuscript Received on 10 october, 2019.

NaganagoudaPatil, Research Scholar, Department of ECE, T John Institute of Technology, Bangalore-560083 and affiliated to Visvesvaraya Technological University,Belagavi,Karnataka, India. (Email: ncpatil@gmail.com)

P V Rao, Professor, Dept of ECE, VBIT, Hyderabad, T.S., India-501301 (Email: raopachara@gmail.com).

commonly not available in major primary healthcare centers. ONH examination is an expedient approach to identify Glaucoma in its early stage, and is contemporarily performed by professional and skilled Glaucoma specialists [4]. Undeniably, manual ONH process is time consuming and even costly [4]. In major ONH methods different morphological or clinical parameters like Vertical Cup to Disc Ratio (CDR), Rim to Disc Area Ratio (RDR), NRR, and Disc Diameter are used to detect and characterize Glaucoma in the fundus images. CDR based methods have been extensively used where a larger CDR signifies higher Glaucoma-risk [3]. However, recent studies reveal that the morphological traits involved in these approaches vary over different demography and populations and hence detecting Glaucoma based on a static threshold can't be the optimal solution. The sophisticated CAD systems for automatic Glaucoma detection involve Region of Interest (ROI) detection and segmentation, features extraction and classification. It uses measurement-based schemes to perform Glaucoma detection [5-9], where at first it localizes the ROI and then obtains features (clinical measurement values) in the fundus images. In such approaches, efficacy of the model depends mainly on the ROI segmentation accuracy. Towards these objectives, different efforts including super-pixel based classifier which functions in conjunction with the different visual features for OD, OC and CDR estimation has been recommended [7][10]. However, maintaining optimal accuracy under different spatial-temporal features of the human eye is intricate. Different complexities like the presence of nerves over the disk surfaces make segmentation difficult. Though, CDR and similar clinical measurements (i.e., RDR, NRR) based methods have been used extensively for Glaucoma detection; however inherent processes like pre-processing, segmentation, post-segmentation, the presence of morphological differences and nerves over the OD region make it more complex and computationally over-burdened [5]. In the last few years, Deep Learning (DL) methods have gained wide-spread attention towards image processing and analysis which has enabled it to be used for different target detection and classification problems [9][15]. To support existing morphological traits based approaches, authors developed a multi-label DL model to segment OD and OC region jointly that helped CDR estimation for Glaucoma detection in fundus images. However, its efficacy remains questionable for a global solution.

Learning-based methods with learned classifiers have been found efficient for Glaucoma detection as these approaches have learnt over the minute features to make eventual decision [11-15]. In DL based schemes the extracted visual features provide more information possessing significant feature-representations than the classical clinical measurements based methods [3]. DL methods have exhibited better performance for generating significant and highly discriminative representations to support a large number of computer vision based applications [20], including medical image analysis [16-18]. Convolutional Neural Networks (CNNs) which is a well recognized and explored deep learning method learns hierarchical features from the input image to make retinal feature such as vessel detection [3][19][20], glaucoma detection [21][22], etc. However, these methods primarily relied on the OD limited contextual information available in the patch and overlooked the global information from the whole fundus image to make more accurate classification. Improper ROI segmentation and OD region cropping too impact overall Glaucoma detection accuracy [3]. CNN as learning technology possess robust learning ability due to its scaling, shifting, translation, manipulation and rotation of the inputs with extreme diversity and non-linearity characteristics, which makes it a suitable too for Glaucoma detection and classification purposes. Additionally, it is designed specifically to analyze and classify visual patterns directly from pixel images without indulging pre-processing and segmentation. It makes it computational efficient. Though, classical CNNs have performed well; however retrieving suitable feature maintaining computational efficacy has remained a challenge. To assist light weight deep leaning process, Auto-Encoder (AE) based approaches have been proposed; however its efficient implementation and architectural design towards the specific problem often needs better strategy. Considering, the efficacy of AE towards Glaucoma detection and classification, in this paper we have designed a novel Stacked Auto-Ender (SAE) based Glaucoma detection and classification system is developed. To further enhance the performance of SAE based model, in this research we applied CNN based SAE, here onwards called CAE. In this paper, we proposed Stacked Auto-Encoder assisted Deep Learning Model for Glaucoma Detection and Classification (GlaucoNet). Our proposed SAE based GlaucoNet model constitutes a deep hierarchical structure to enable better and deep feature extraction so as to ensure better detection and classification. As structural design, our proposed model implements dual-stage SAE with two convolutional layers, max-pool and Fully Connected layers. In addition, we employed cascaded SAE with ReLU normalization, dropout (50%) to achieve computational efficacy. The overall MATLAB based simulation model is assessed with two benchmark datasets, DRION-DB and DRISHTI-GS. Performance assessment in terms of accuracy, precision, F-Measure, Recall etc have exhibited that the proposed model outperforms other state-of-art techniques.

The remaining sections of the presented manuscript are divided as follows: Section II discusses the related work, which is followed by the preliminaries and proposed methods in Section III. Section IV presents system implementation while the results obtained are discussed in Section V. Overall research conclusion and future scopes are discussed in Section VI. References used are mentioned at the end of the manuscript.

II. RELATED WORK

Yousefi, et. al., proposed a hierarchical model comprising clustering, glaucoma boundary and its progression detection to identify the glaucomatous visual field defect patterns and its progression. In [24], authors at first detected Retina Nerve Fiber Layer Defect (RNFLD) in fundus images using

patch features driven Recurrent Neural Network (RNN); however it could not address the other morphological variations like OD or OC . Şahin, et. al., too focused onRNFL thickness detection using Optical Coherence Tomography (OCT) images for glaucoma detection. However, inclusions of the features like optical disk and optical cup morphology could have enabled better performance. The classical methods employ multi-phase mechanism where at first it performs ROI (optical cup, optical disk and blood vessels) detection followed by feature extraction and classification. Though, static threshold based method often gives inaccurate prediction over fundus images of different patients, authors suggested applying adaptive threshold based ROI detection (blood vessels), Gabor filter and Top-Hat transform based feature extraction, and Extreme Learning Machine (ELM) based classification to perform Glaucoma detection. However, ensuring optimal feature extraction and further classification remains an open research area. With this motive, authors applied inpainting concept to perform accurate ROI feature extraction by applying circular Hough transform. In authors exploited Hybrid Structural Features (HSF) as well as hybrid textural features (HTF) which were further processed using Support Vector Machine (SVM) classifier to classify fundus images as normal or Glaucomatic. Unlike conventional ROI detection, authors applied super-pixels algorithm for detecting damaged cup. In [28], authors applied Hough transformation to perform feature extraction from OD in the fundus image. A hybrid level-set algorithm based OD and OC detection was performed in to perform Glaucoma detection. Unlike thresholding based approaches, authors applied region growing concept to detect OD in retinal fundus images. To exploit multiple morphological features of the fundus images, authors extracted features like vertical CDR, Horizontal to Vertical CDR (H-V CDR), Cup to Disc Area Ratio (CDAR), and Rim to Disc Area Ratio (RDAR) to perform Glaucoma detection. CDR as ROI was also applied in to perform Glaucoma detection. However, in major CDR based approaches, authors didn't consider segmentation error and its impact on classification accuracy. To alleviate it, authors introduced Polar transform assisted unsupervised algorithm for OC segmentation. Unlike above stated approaches where morphological trait and distance information is applied, authors applied polar coordinate information to detect ROI. Additionally, authors applied watershed transform for feature extraction from CDR and NRR. The extracted features from the CDR and NRR ROI were used as input to the SVM for two-class classification (i.e., glaucoma and non-glaucoma). In authors used simple linear iterative clustering (SLIC) for ROI detection, which was followed by feed-forward neural network based classification for Glaucoma detection and classification. Extracting CDR features authors [42], applied K-Mean clustering algorithm to perform Glaucoma detection.

To enhance computation, authors recommended extracting a section of the eye sclera and estimated its percentage to detect Glaucoma in funds images. However, its performance can't be generalized as the aforesaid trait might vary over one to another. In [36][37], a self assessed disc segmentation method was proposed for OD and OC segmentation [44], where deriving CDR values in the fundus image authors performed Glaucoma detection. However, the use of static CDR threshold for classification limits its generalization. Authors applied edge detection model using GVF Snake Active Contour. As preprocessing authors applied 2D median filter and Multi threshold methods. Researches [38-43] state that the majority of classical CDR based approaches suffer inaccuracy in prediction, especially in OC detection over the horizontally identified disk region that makes overall detection output suspicious. In [45], authors pre-processed input with filtering, green channel extraction and CLAHE implementation to achieve better CDR estimation. Further, they used active contour propagation based blood vessel segmentation to enhance CDR estimation accuracy [46][47]. In [48], authors estimated OD center using thresholding and distance transformation, which was then followed by the estimation of Eigenvector spaces of normal set and glaucoma using Principle Component Analysis (PCA) algorithm. Authors applied Bayes classifier. GLCM features were applied in [49], which was classified using Logistic Regression classifier to classify fundus-image as normal or Glaucomatic. Unlike morphology factors, authors applied color and texture features from the blood vessel to perform glaucoma detection. In Haralick texture features were obtained from fundus images which were later classified using K Nearest Neighbors (KNN) classifiers to perform glaucoma detection. To reduce segmentation and allied complexities, authors suggested deep learning method that exploits image-relevant information and classifies glaucoma from the fundus images. In [53], authors applied G-EyeNet a deep learning model comprising a deep CAE model to perform Glaucoma detection. In as well authors applied CNN to perform automated Glaucoma detection. A pre-trained CNN based automatic target detection scheme was developed in [55]. Authors too proposed the detection of OD and OC by using deep learning and CNNs.

III. PROPOSED SYSTEM

To enable a robust and efficient automatic Glaucoma detection and classification model, in this paper, we have proposed a novel Stacked Auto-Encoder (SAE) assisted CNN model. It inherits the functional characteristics of the Convolutional Auto-Encoders to perform Glaucoma detection and classification. As contribution, the proposed SAE model embodies stacked SAE implementation along with hierarchical CNN, which makes it robust to perform optimal deep feature extraction, learning and classification. Unlike classical CNNs, GlaucoNet incorporates SAE structure which is a CAE model that extracts deep features sequentially and combines multiple features to make further classification. Structurally, it embodies 3 Convolutional layers (CONV) and 2 Fully Connected (FC) layers, where the CONV extracts the features and learns over it, while FC layers functions as the classification layer to perform two-class classification, Glaucomatic and Non-Glaucomatic fundus images.

To avoid convergence and maintain low computational overhead, we applied dropout concept that in conjunction with ReLu Non-linearity and local response normalization enabled overall process computationally efficient and accurate. GlaucoNet has been examined for its detection and classification efficiency over two well known datasets, DRISHTI-GS and DRION-DB, where the performance is assessed in terms of accuracy, precision, recall, f-measure etc. The detailed discussion of the proposed model is given in the sub-sequent sections.

A. Auto-Encoder(AE)

AEs are a type of unsupervised learning model that considers an input $x \in R^d$ to map it for deriving the latent representation $h \in R^{d'}$. It is achieved by using a deterministic function $h = f_\theta = \sigma(W_x + b)$ with parameters $\theta = \{W, b\}$, where W and b state the weight and the bias values, respectively. In later phase, it executes reverse mapping of the function f so as to reconstruct the input data and thus it obtains the reconstructed feature as $y = f_{\theta'}(h) = \sigma(W'h + b')$. To perform encoding and decoding two parameters are typically conditioned to satisfy $W' = W^T$ by applying similar weights. All training patterns x_i are mapped distinctly onto its code h_i and allied reconstructiony_i, while the parameters are augmented by reducing certain suitable cost function over the training set $D_n = \{(x_0, t_0), \ldots, (x_n, t_n)\}$. An AE learns the mapping without applying any additional constraints; however to achieve better accuracy over non-linear mapping patterns it requires methods like probabilistic Boltzman machine (RBM) or sparse coding, or sometime the de-noising AEs (DAs) to reconstruct input data under noise. Amongst these approaches DA performs better and hence we have applied it to constitute a hierarchical learning model. Generally, fundus images might have different spatio-temporal noises and therefore DA can reconstruct a clean input from a partially destroyed fundus images. Let, a fundus image $x$be corrupted ($\bar{x}$)due to certain noise inclusion, then AE can be trained to *de-noise* the inputs by estimating the latent representation $h = f_{\theta'}(\bar{x}) = \sigma(W\bar{x} + b)$and thus enables original image reconstruction output $y = f_{\theta'}(h) = \sigma(W'h + b')$. In GlaucoNet, AE functions as Hierarchical Feature Extractor (HFE) that scales input fundus images to the high-dimensional features for further analysis and classification. To perform feature learning, Scale Conjugate Gradient Algorithm (SCGA) is applied. Relearning the features extracted from AE by sequentially forward-placed AE can help obtaining more vital and deep features for better classification accuracy. Considering it as motivation, we designed a robust SAE architecture for deep feature extraction and learning for Glaucoma classification. A snippet of the SAE model is given as follows:

B. Stacked Auto-Encoder (SAE)

Here, to design a SAE model, we stacked multiple AEs in cascade fashion that formed a deep hierarchical model. In this approach, each layer obtains its input from the latent representation of the previous layer. In GalucoNet as well, multiple layers of the AEs are connected in such manner that the output of each layer is connected to the input layer. In our proposed SAE model sparsity feature has been incorporated that reduces the reconstruction error swiftly. Let, SAE has n layers with $\mathrm{W}^{(k,1)}$, $\mathrm{W}^{(k,2)}$, $\mathrm{b}^{(k,1)}$, $\mathrm{b}^{(k,2)}$, where $\mathrm{W}^{(k,1)}, \mathrm{W}^{(k,2)}$, $\mathrm{b}^{(k,1)}$, $\mathrm{b}^{(k,2)}$ be the weights and bias values for the k-th AE. In AE, encoding of the each layer in the forward order is given as (1-2).

$$a^{(l)} = f\left(z^{(l)}\right) \quad (1)$$

$$z^{(l+1)} = W^{(l,1)}a^{(1)} + b^{(l+1)} \quad (2)$$

On contrary, the decoding part of each layer employs reverse order functions as depicted in (3-4).

$$a^{(n+l)} = f\left(z^{(n+l)}\right) \quad (3)$$

$$z^{(n+l+1)} = \mathrm{W}^{(n-l,2)}\mathrm{a}^{(n+l)} + \mathrm{b}^{(n-l+2)} \quad (4)$$

Here, higher order features are extracted from the vector presentation of the input fundus images and significant information is stored in $a^{(n)}$.It is further used to perform classification by feeding it to a Softmax classifier as a multiclass classifier (i.e., Glaucomatous or Non-Glaucomatous). In GlaucoNet, Softmax primarily maps the value of the input vector to a real value possessing redundant characteristics of the parameters. To achieve it, the first layer possessing the raw input of parameters$\mathrm{W}^{(1,1)}, \mathrm{W}^{(1,2)}$, $\mathrm{b}^{(1,1)}$, $\mathrm{b}^{(1,2)}$ is trained and thus the raw input is transformed to a vector comprising activation of the hidden units. In the later phase, the second layer AE is trained by estimating $\mathrm{W}^{(2,1)}, \mathrm{W}^{(2,2)}, \mathrm{b}^{(1,1)}, \mathrm{b}^{(1,2)}$. This process is continued repeatedly by applying the output of each layer as the input for the subsequent layer. Noticeably, in this paper we used two layers of the AE to form SAE design. During learning we applied learning method named Stochastic Gradient Descent (SGD) that tunes the parameters to achieve optimal results..

Unlike conventional approaches where single AE is applied as solution, in our proposed GalucoNet model we have applied a hierarchical approach where obtaining the 2 level SAE features, we have implemented a CNN deep learning approach that inherits the SAE extracted features and cascades its own extracted features to yield a combined feature set for further classification. The detailed discussion of CNN model is given as follows:

C. Convolutional Neural Networks (CNN)

In GlaucoNet, the encoded feature is given as input to the CNN that employs a sequence of layers including Convolutional Layers (CONV), Max-pooling or Pooling Layers, and Fully-Connected (FC) Layers to perform feature extraction and learning.

I. Convolutional Layer (CONV)

CONV can be stated as the combination of filters which are capable of extracting certain specific patterns or features from the input image. In our case, CONV extracts the features from the funds images which are obtained as the output. Each neuron in the extracted feature map shares similar set of weights (W) and bias (b) values to enable neurons in a feature map detecting the similar feature. Similarly, the other feature maps in CONV employ different

sets of biases and weights to enable extraction of the different local features.

II. Max-Pooling Layer

Once retrieving the CONV features, CNN applies pooling layer that functions as feature selection layers where it sequentially minimizes the spatial resolution of each feature map. Additionally, it minimizes the number of parameters and computation required by using local averaging and a sub-sampling technique that eventually avoids the problem of over-fitting. In our proposed model, we applied native Max-pooling that helped retrieving translation-invariant representations s by down-sampling the significant latent representation from the fundus images using a constant component by considering the highest value over non-overlapping segments or sub-regions. We applied Max-pooling in such manner that it functions as an optimal filter to select important features for further classification. It was possible because the similarity between the features and the ROI (i.e., the input field) defines the activation of each neuron in the latent representation. Additionally, it considers sparsity over the hidden representation by removing all non-maximal values in certain non overlapping sub-space and thus enhances feature detectors to avoid insignificant solutions. During reconstruction, the derived sparse latent code reduces number of filters to decode each pixel and hence makes it more suitable for Glaucoma detection and classification. Recalling SAE structure ad discussed in previous section, in GlaucoNet, SAE acts as initializing unit for CNN with similar topology before executing supervised training. Once obtaining the cumulative features, our model maps extracted and selected features to the Fully Connected layer.

III. Fully-Connected Layer (FC)

FC layers functions at the end of the CNN to perform high-level reasoning tasks or classification. It receives a set of neurons, also called feature vector from the preceding layer and maps it to all connected neurons to generate a one-dimensional (feature) vector. It supports CNN to perform image analysis and classification easily. In GlaucoNet model we have performed classification by reducing an objective function.

D. Convolutional Stacked Auto-Encoder (CSAE)

Observing above stated details or the proposed method, it can be observed that the proposed GalucoNet model embodies strengths of both CAE as well as CNN and hence we rename it as Convolutional Stacked Auto-Encoder (CSAE). In our proposed CASE instead of using manually engineered convolution filter, we strengthen CNN to learn the optimal filter that reduces the reconstruction error significantly and hence achieves better accuracy. Since, in our proposed method, the optimal filters are applied as feature for CNN to perform training, it can be considered as a feature extraction tool. Unlike classical FC configuration, AEs don't emphasize on the 2D image structure and therefore when dealing with real-time applications such as at hand Glaucoma detection and classification there is the need for fine grained feature. Additionally, it demands each feature to be global or to be distributed across the visual field to make classification; however in Glaucoma detection, ROI can be confined to a specific location and hence detecting localized features is must. Therefore, as already discussed our proposed GalucoNet model with CSAE has been designed in such manner that it shares its weight parameters among all locations in the input fundus images and hence preserves spatial locality to make accurate detection and classification. In conjunction with the derivations done in the previous sub-section, for a mono-channel fundus image or input x the latent representation of the i-th feature map is obtained by (5).

$$h^i = \sigma(x * W^i + b^i) \tag{5}$$

In (5) the parameter b signifies the bias value which is shared across the map, σ refers an activation function, while * representation the 2D convolution. In CSAE single bias per latent map is considered to enable each filter learning the features of whole fundus data. Additionally, it (i.e., a single bias per pixel) helps achieving significantly high degrees of freedom (DoF) and hence better feature learning for more accurate Glaucoma detection and classification. In our proposed CSAE model, reconstruction is performed using (6).

$$y = \sigma\left(\sum_{k \in H} h^i * \bar{W}^i + c\right) \tag{6}$$

As depicted in (6), to reconstruct feature single bias c is applied for each input channel . Here, H signifies the set of latent feature maps , while $\bar{W}$ performs flipping over both dimensions of the weights. The 2D convolution in (5) and (6) is estimated by context. As stated, we applied an objective function which is reduced when learning to achieve optimal learning output. Here, we used Mean Squared Error (MSE) (8) as the objective function is to achieve better and accurate learning. Mathematically,

$$y = \sigma\left(\sum_{k \in H} h^i * \bar{W}^i + c\right) \tag{7}$$

$$E(\theta) = \frac{1}{2n}\sum_{i=1}^{n}(x_i - y_i)^2 \tag{8}$$

Here, we have applied Scale Conjugate Gradient Algorithm to estimate the gradient of the error function. Mathematically, it is achieved by convolution as per (9).

$$\frac{\partial E(\theta)}{\partial W^k} = x * \delta h^k + \bar{h}^k * \delta y \tag{9}$$

In (9), δh signifies the gradient of the hidden state while δy signifies the gradient (i.e., deltas) of the reconstruction and the weights are updated using stochastic SCGA algorithm.

In addition to the above stated approaches; in this work an effort is made few enhancements in ReLu to deal with Non-linearity, and local response normalization that makes overall computation efficient and robust to perform Glaucoma detection and classification.

E. ReLu Non-linearity and local response normalization

Typically, to design a CNN with the neuron's output f as the function of input parameter x two methods, f(x)=tanh⁡(x) or f(x)= 〖(1+e^(-x))〗 ^(-1) are considered. Considering training time with classical Gradient Descent (GD) algorithm, the saturating nonlinearities often used to be slower than the non-saturating nonlinearity f(x)=max⁡(0;x). In major approaches before segmentation and feature extraction normalization is performed to avoid saturation. However, it imposes significantly large computational overheads. To avoid it, we applied ReLu especially to avoid input normalization. In GlaucoNet the neurons with nonlinearity are considered as the ReLu activation function that enables time-efficient training as compared to the classical tanh unit based approach. It has also been found that the nonlinearity in case of hyperbolic tangent functionsf(x)=|tanh(x)| is suitable with certain limited approaches applying contrast normalization followed by local average pooling. However, it suffers over-fitting over learning period. In such case the implementation of our proposed ReLu model and local response normalization achieves better performance and it can cope up with the accelerated ability to fit the training set efficiently. Thus, the augmented learning method enables GlaucoNet to be used even with the large number of input datasets. Functionally, when a part of training samples generate a positive input to a ReLu, it triggers learning in that neuron. Let 〖a^i〗 _(x,y) be the neuron's activity obtained using i-th kernel at location(x,y). Now, ReLu nonlinearity estimates the response-normalized activity 〖b^i〗 _(x,y) using (10).

$$b^{i}{}_{x,y} = \frac{a^{i}{}_{x,y}}{\left(K + \alpha \sum_{j-\max\left(0,i-n/2\right)}^{\min\left(N-1,i+n/2\right)} \left(a^{i}{}_{x,y}\right)^{2}\right)^{\beta}} \qquad (10)$$

In (10), the sum continues over n "adjacent" kernel maps at the same spatial position, while N signifies the total available kernels in that layer. Typically, the mapping or ordering of the kernel maps is random which is decided before executing training. Such kind of response normalization applies a type of lateral inhibition motivated by the specific type present in real neurons, thus constituting competition for big activities among the neurons outcomes estimated by the different kernels. In above equation the constant parameters k,n,α and β signify the hyper-parameters which are usually estimated using a validation set. Here, in this paper we applied k = 2, n = 5, α= 〖10〗 ^(-4), and β=0.75. We used this normalization once executing the ReLu nonlinearity in layers.

IV. RESULTS AND DISCUSSION

Though, AEs based methods have been used for Glaucoma detection in the existing literatures, their performance especially in terms of accuracy, recall, Receiver Operating Characteristics (ROC), remained low. This could be primarily due to low feature extraction under fine-grained non-linear fundus image characteristics. Considering such limitations, in this paper Stacked Auto-Encoder assisted CNN is designed for Glaucoma detection in fundus images. Unlike conventional Auto-Encoders the proposed Stacked Auto-Encoder based CNN concatenates multiple Auto-Encoders in series to constitute a deep hierarchy for feature extraction followed by entropy based classification. The proposed SAE comprises the encoder and the decoder paths, where each encoder path exhibits convolutional layer (CONV) with a distinct filter bank to generate a set of encoder feature maps. Noticeably, to achieve it we applied element-wise rectified-linear non-linearity (ReLu) activation function. On the contrary, the decoder path employed CONV layer to generate the decoder feature map. Here, the skip connections transfer the subsequent feature map from encoder path and concatenate it to up-sampled decoder feature maps. Eventually, a classifier employs 2×2 CONV layer with sigmoid activation function as the pixel-wise classification to generate map for the Glaucoma presence. Furthermore, a new branch was extended from the saddle layer that functions as an implicit vector with average pooling. In the next step, it joins two FC layers so as to generate the Glaucoma classification likelihood. In fact this approach embeds the segmentation-guided representation by means of the CONV filters on the decoder path. In this paper, the input images were resized to 256×256 dimension while retaining the significant information for ROI localization and further classification. Noticeably, we used Binary Cross Entropy (BCE) as the loss function to perform classification. The employed loss function was integrated in a back-propagation manner using Stochastic Gradient Descent (SGD) or SCGA algorithms. Eventually, the CNN parameters were frozen, which was then followed by training of the FC layers using Glaucoma detection training data (here, DRISHTI dataset). Noticeably, we used training rate gamma as 0.0001, while the droprate was fixed at 0.5 (50%).

A. Datasets

Considering the fact that different benchmark datasets (i.e., fundus images) used to have the different spatio-temporal features and therefore assessment of the proposed model with the different benchmarks (dataset) can give better performance visualization. With this motive, in this research two distinct datasets, DRION-DB and DRISTHI-GS were taken into consideration. In case of the DRISHTI-GS datasets a total of 100 fundus images were used for training, while a total of 50 images were used for testing or validation. Similarly, for DRION-DB datasets, a total of 110 fundus images were used for training while, 50 images were used for testing. The considered fundus images were having different characteristics including lighting conditions, OD and OC position, nerve presence etc. Noticeably, the considered images wee encompassing both glaucomatous eyes images as well as normal images to assess efficacy of the proposed Glaucoma detection and classification system. The images were processed for 256×256 dimension before performing feature localization and allied feature extraction. Table I.a) presents a snippet of the Glaucoma fundus datasets and Table 1.b samples fundus images pertaining to DRION-DB and DRISHTI-GS datasets used in this research. The number of images used for both training and testing is given in Table II.

Table I.a Samples of the different Fundus images

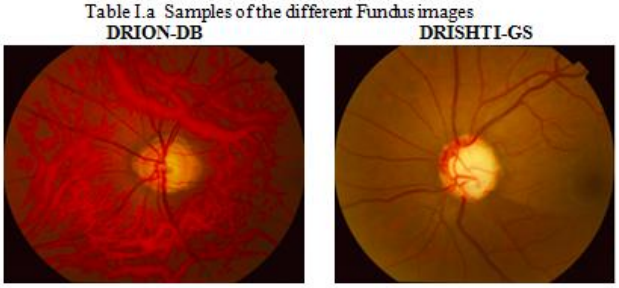

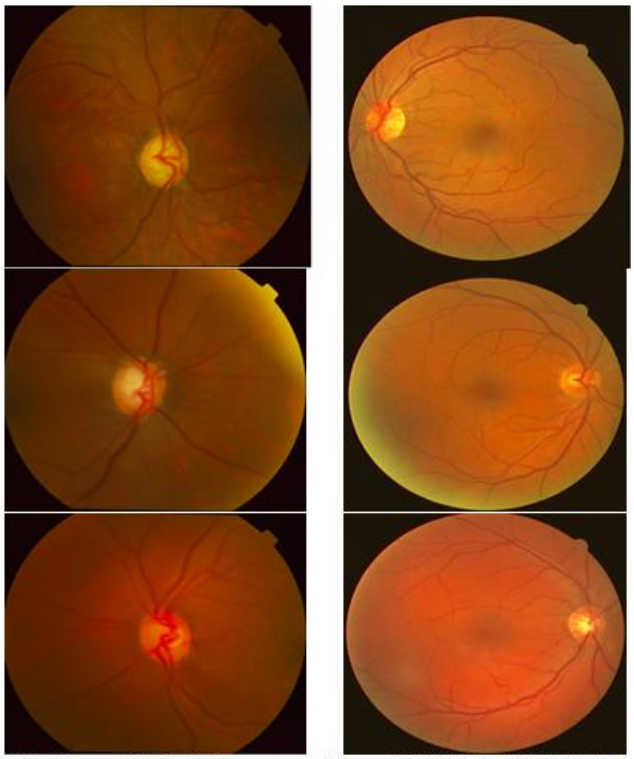

Table 1.b samples fundus images pertaining to DRION-DB and DRISHTI-GS datasets

Table II Datasets for performance assessment

Datasets	Specification	
DRISHTI-GS	Training	100
	Testing	50
DRION-DB	Training	110
	Testing	50

Performance Evaluation

To examine performance efficiency of the proposed Stacked Auto-Encoder based Glaucoma detection and classification system different performance matrix such as true positive (TP), true negative (TN), false positive (FP) and false negative (FN) have been obtained. Further, these matrix values have been used to obtain Accuracy, Precision, F-Measure, Recall, Balanced Accuracy, ROC etc. Here, we considered Balanced Accuracy (BACC) as the average of sensitivity and specificity so as to accommodate data imbalance scenario (i.e., the number of positive and negative cases) in the testing data set. The ROC graph has been obtained to depict the two-dimensional representation with the Sensitivity (Y-axis) and Specificity (X-axis). The definitions of these performance variables are given in Table III.

Table III Performance Parameters or Criteria

Parameter	Mathematical Expression
Accuracy	$\frac{(TN+TP)}{(TN+FN+FP+TP)}$
Precision	$\frac{TP}{(TP+FP)}$
F-measure	$2.\frac{Recall.Precision}{Recall+Precision}$
Recall or Sensitivity	$\frac{TP}{(TP+FN)}$
Balanced Accuracy	$\left(\frac{\text{Recall} + \text{Specificity}}{2}\right)$

The performance parameters and their respective values are given in Table IV.

Table IV Performance of GlaucoNet

	DRISHTI-GS	DRION-DB
	Performance (%)	Performance (%)
Accuracy	98.2	96.3
Precision	94.6	93.9
F-Measure	97.9	94.1
Recall -Sensitivity	99.6	94.2
Specificity	94.6	92.6
BACC	97.1	93.4
AUC	0.94	0.90

The graphical depiction of the performance by our proposed Glaucoma detection and classification system for DRISHTI-GS and DRION-DB datasets is given in Fig.

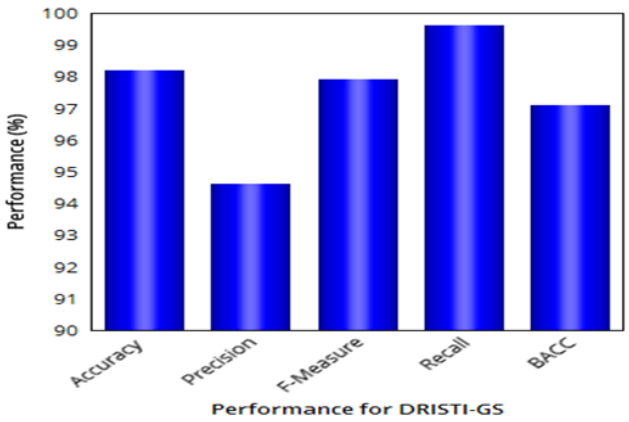

Fig. 1 Performance analysis with DRISHTI-GS1 dataset

As stated above, to assess performance of the propose Glaucoma detection system, two distinct benchmark datasets DRISHTI-GS and DRION-DB have been considered. Considering diversity across the different datasets and allied complexity, the performance characterization for these two different data can depict better efficacy of the proposed model. Observing the results it can be found that the proposed Stacked Auto-Encoder assisted CNN model exhibits 98.2% of the accuracy with DRISHTI-GS dataset. Similarly, it has exhibited precision of 94.6% and F-Measure of 97.9%. Interestingly, the recall performance has been obtained as 100 %. Similarly, it has exhibited 96.3% of accuracy with almost 94% of the precision and 94.1% F-Measure.

Considering the probable imbalance issue during training and testing, we have estimated Balanced Accuracy (BACC). In this research we observed that the BACC values for DRISHTI-GS and DRION-DB datasets were 97.1% and 93.4%, respectively. The Area under Curve (AUC) obtained with these datasets were 0.94 and 0.90 that signifies satisfactory performance over the state of art classical CDR, NRR and conventional CNN based approaches.

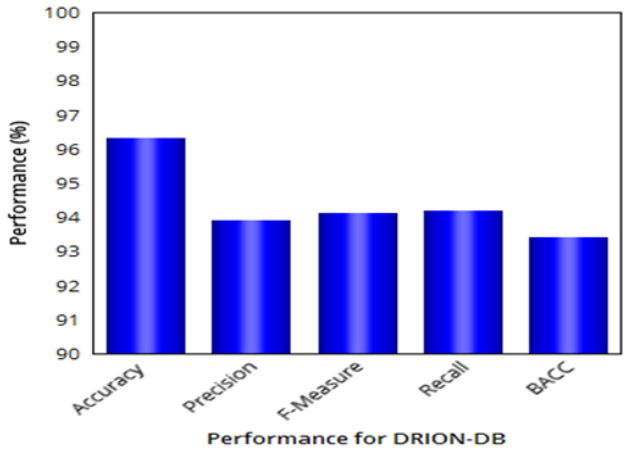

Fig. 2 Performance analysis with DRION-DB dataset

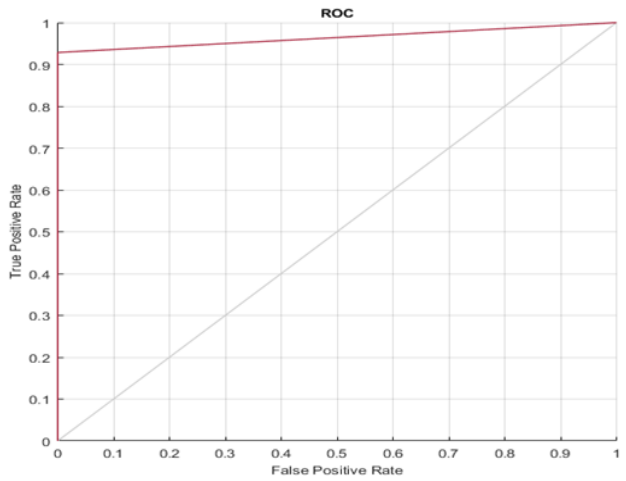

Fig.3 ROC performance for DRISHTI-GS dataset

Observing the above stated results, it can be found that the proposed GlaucoNet model outperforms existing state-of-art techniques. As illustration for qualitative assessment, a comparison chart for the different existing methods and approaches applied is given in Table V.

Author	Detection/Segmentation	Classification
[3]	OD Information	Ensemble Learning
[5]	OD and OC based Segmentation	-
[6]	Model-based optic nerve head segmentation	-
[7]	OD and OC	Superpixel classification
[8]	OD	Quadratic divergence regularized SVM
[9]	Joint OD and OC Segmentation Based on Multi-label Deep Network and Polar Transformation	-
12	Wavelet-based energy features	-
[13]	High order cumulant features	-
[14]	Gabor transformation	-
[21][22]	-	Automatic Feature Learning for Glaucoma Detection Based on Deep Learning
[24]	RNN based Retinal Nerve Fiber layer defect detection	-
[25]	Retinal Nerve Fiber Layer detection	-
[26]	OD segmentation using circular Hough transform and curve fitting	-
[27]	Hybrid structural and textural features	-
[28]	Glaucoma detection using texture features extraction	-
[29]	OD detection in high-resolution retinal fundus images by region growing	-
[32]	Polar Space Contour Detection for Automated OC egmentation	-
[33]	Neuroretinal Rim information	-
[34][36] [41][42] [44]	Measurement of optical CDR	-
[35]	Determination for Glaucoma disease based on red area percentage	-
[43]	GVF Snake Active Contour method and Ellipse Fit in OD detection for glaucoma diagnosis	-
[46]	Super pixels from fundus colour retinal images	-
[49]	GLCM techniques	Logistic Regression classifier
[50]	Color and Texture Features	-
[51]	Haralick texture features	-
[52]	Disc-Information	Ensemble Network
[53]	-	Convolutional Autoencoding Classifier
[54]	-	CNN
[55]	Optic Disc Detection Using Fine Tuned Convolutional Neural Networks	-
		-
[57]	Fuzzy based decision making for detection of Glaucoma	Fuzzy logic
[58]	Intraocular pressure monitoring	-
[59]	Wavelet energy features	ANN
[60]	OC and OD	K-mean clustering
[63]	Retinal layers segmentation and OCDR	-
[64]	OD segmentation using morphological techniques and active contour fitting	-
[66]	cup-disk and rim-disk ratio	-
Proposed Galuco Net	-	CSAE Hierarchical CNN model

	Accuracy	Precision	F-Measure	BACC	Recall (	Specificity	AUC
[3]				0.8429	0.8478	0.838	0.9183
[27]	100.00	-	-	-	94.00	-	-
[28]	84.0	-	-	-	-	-	-
[29]	-	-	-	-	98.60	97.20	-
[30]	99.20	-	-	-	86.00	84.00	-
[33]	94.10	-	-	-	91.80		
[34]	-	-	-	-	92.00	88.00	
[38]	97.50	-	-	-	-	-	
[41]	80.00	-	-	-	95.00	91.00	-
[42]	97.00	-	-	-	-	-	-
[43]	84.38	-	-	-	-	-	-
[48]	95.50	-	-	-	-	-	-
[49]	88.7	-	-	-	60.6	70.3	-
[51]	98	-	-	-	-	-	-
[53]	-	-	-	-	-	-	0.923
[54]		-	-	-	-	-	0.831
[56]	93.00	-	-	-	-	-	-
[57]	88.00	-	-	-	-	-	-
[58]	-	-	-	-	-	-	81.50
[59]	89.6 (NB) 97.6 (ANN)	-	-	-	-	-	-
[60]	92.00	-	-	-	-	-	
[61]	-	-	-	-	-	-	0.96
[62]	72.38	-	-	-	-	-	0.79
[63]	79.00	-	-	-	87.00	72.00	
[64]	83.10	-	-	-	-	-	-
[65]	92.00	-	-	-	-	-	-
[66]	90.00	-	-	-	-	-	-
DRISHTI-GS	**98.2**	**94.6**	**97.9**	**97.1**	**99.6**	**94.6**	**0.94**
DRION-DB	**96.3**	**93.9**	**94.1**	**93.4**	**94.2**	**92.6**	**0.90**

V. CONCLUSION

In this paper a highly robust and enhanced Stacked Auto-Encoder assisted CNN model has been developed for Glaucoma detection and classification in fundus images. Unlike conventional approaches where authors have applied pre-processing, segmentation, post segmentation, feature extraction, classification etc, the proposed system which is named as GlaucoNet avoids above stated processes and performs feature extraction using Stacked Auto-Encoder. The extracted features are pooled and later classified to perform two class classification, Glaucomatic image and normal image. Unlike classical Auto-Encoder, authors designed Stacked Auto-Encoder which extracts deep features and forms deep hierarchical convolutional network to perform Glaucoma detection and classification. This approach has enabled higher accuracy without incorporating more computational overheads. GlaucoNet model comprises three-convolutional layer, followed by Max-pooling and Fully-Connected layers, where the CONV layers use filters to extract high dimensional features in conjunctional with the ReLU activation function. The use of dropout (0.5) has avoided the issue of over-fitting which is common in major CNNs or machine learning approaches. The MATLAB based simulation has revealed that the proposed GlaucoNet model achieves classification accuracy of 98.2% and 96.3% for DRISHTI-GS and DRION-DB datasets, respectively. In addition, it has exhibited Balanced Accuracy (BACC) of 97.1% and 93.4% for DRISHTI-GS and DRION-DB. AUC of 0.94 and 0.90 for the considered datasets affirms robustness and efficacy of the proposed Glaucoma detection and classification system.

VI. ACKNOWLEDGEMENT

We gratefully thank the Visvesvaraya Technological University, Jnana sangama, Belagavi for financial support extended to this research work. Secondly Sincere Thanks to my supervisor for providing constant and concurrent support for utilization of computational facilities by FIST grant of DST, VBIT, Ghatkesar, T.S., India, during the progress of this work

REFERENCES

1. Y.-C. Tham, X. Li, T. Y. Wong, H. A. Quigley, T. Aung, and C.-Y. Cheng, “Global prevalence of glaucoma and projections of glaucoma burden through 2040: A systematic review and meta-analysis,” Ophthalmology, vol. 121, no. 11, pp. 2081–2090, 2014.
2. S. Y. Shen, T. Y. Wong, P. J. Foster, J.-L. Loo, M. Rosman, S.-C. Loon, W. L. Wong, S.-M. Saw, and T. Aung, “The prevalence and types of glaucoma in malay people: The singapore malay eye study,” Investigative Ophthalmology and Visual Science, vol. 49, no. 9, p. 3846, 2008.
3. H. Fu et al., "Disc-Aware Ensemble Network for Glaucoma Screening From Fundus Image," in IEEE Transactions on Medical Imaging, vol. 37, no. 11, pp. 2493-2501, Nov. 2018.
4. H. Fu, Y. Xu, S. Lin, X. Zhang, D. Wong, J. Liu, and A. Frangi, “Segmentation and Quantification for Angle-Closure Glaucoma Assessment in Anterior Segment OCT,” IEEE Trans. Med. Imag., vol. 36, no. 9, pp. 1930–1938, 2017.
5. G. D. Joshi, J. Sivaswamy, and S. R. Krishnadas, “Optic Disk and Cup Segmentation from Monocular Colour Retinal Images for Glaucoma Assessment,” IEEE Trans. Med. Imag., vol. 30, no. 6, pp. 1192–1205, 2011.
6. F. Yin, J. Liu, S. H. Ong, Y. Sun, D. W. K. Wong, N. M. Tan, C. Cheung, M. Baskaran, T. Aung, and T. Y. Wong, “Model-based optic nerve head segmentation on retinal fundus images,” in Proc. EMBC, 2011, pp. 2626–2629.
7. J. Cheng, J. Liu, Y. Xu, F. Yin, D. Wong, N. Tan, D. Tao, C.-Y. Cheng, T. Aung, and T. Wong, “Superpixel classification based optic disc and optic cup segmentation for glaucoma screening,” IEEE Trans. Med. Imag., vol. 32, no. 6, pp. 1019–1032, 2013.
8. J. Cheng, D. Tao, D. W. K. Wong, and J. Liu, “Quadratic divergence regularized SVM for optic disc segmentation,” Biomed. Opt. Express, vol. 8, no. 5, pp. 2687–2696, 2017.
9. H. Fu, J. Cheng, Y. Xu, D. Wong, J. Liu, and X. Cao, “Joint Optic Disc and Cup Segmentation Based on Multi-label Deep Network and Polar Transformation,” IEEE Trans. Med. Imag., 2018.
10. [10 J. Cheng, F. Yin, D. W. K. Wong, D. Tao, and J. Liu, “Sparse dissimilarity-constrained coding for glaucoma screening,” vol. 62, no. 5, pp. 1395–1403, 2015.
11. R. Bock, J. Meier, L. G. Nyul, J. Hornegger, and G. Michelson, “Glaucoma risk index: Automated glaucoma detection from color fundus images,” Medical Image Analysis, vol. 14, no. 3, pp. 471–481, 2010.
12. S. Dua, U. Rajendra Acharya, P. Chowriappa, and S. Vinitha Sree, “Wavelet-based energy features for glaucomatous image classification,” IEEE Transactions on Information Technology in Biomedicine, vol. 16, no. 1, pp. 80–87, 2012.
13. K. P. Noronha, U. R. Acharya, K. P. Nayak, R. J. Martis, and S. V. Bhandary, “Automated classification of glaucoma stages using higher order cumulant features,” Biomedical Signal Processing and Control, vol. 10, no. 1, pp. 174–183, 2014.
14. U. R. Acharya, E. Ng, W. Eugene, Lim, K. Noronha, L. Min, K. Nayak, and S. Bhandary, “Decision support system for the glaucoma using Gabor transformation,” Biomedical Signal Processing and Control, vol. 15, pp. 18–26, 2015.
15. A. Krizhevsky, I. Sutskever, and G. Hinton, “Imagenet classification with deep convolutional neural networks,” in Proc. NIPS, 2012, pp. 1097–1105.

16. V. Gulshan, L. Peng, M. Coram, and et.al, “Development and Validation of a Deep Learning Algorithm for Detection of Diabetic Retinopathy in Retinal Fundus Photographs,” Journal of the American Medical Association, vol. 304, no. 6, pp. 649–656, 2016.
17. A. Esteva, B. Kuprel, R. A. Novoa, J. Ko, S. M. Swetter, H. M. Blau, and S. Thrun, “Dermatologist-level classification of skin cancer with deep neural networks,” Nature, vol. 542, no. 7639, pp. 115–118, 2017.
18. D. Shu Wei Ting and et al., “Development and Validation of a Deep Learning System for Diabetic Retinopathy and Related Eye Diseases Using Retinal Images From Multiethnic Populations With Diabetes,” JAMA, vol. 318, no. 22, pp. 2211–2223, 2017.
19. Q. Li, B. Feng, L. Xie, P. Liang, H. Zhang, and T. Wang, “A Cross modality Learning Approach for Vessel Segmentation in Retinal Images,” IEEE Trans. Med. Imag., vol. 35, no. 1, pp. 109–118, 2016.
20. H. Fu, Y. Xu, S. Lin, D. W. K. Wong, and J. Liu, “DeepVessel: Retinal Vessel Segmentation via Deep Learning and Conditional Random Field,” in Proc. MICCAI, 2016, pp. 132–139.
21. X. Chen, Y. Xu, S. Yan, D. Wing, T. Wong, and J. Liu, “Automatic Feature Learning for Glaucoma Detection Based on Deep Learning,” in Proc. MICCAI, 2015, pp. 669–677.
22. J. I. Orlando, E. Prokofyeva, M. Del Fresno, and M. B. Blaschko, “Convolutional neural network transfer for automated glaucoma identification,” in Proc. SPIE, 12th International Symposium on Medical Information Processing and Analysis, 2016.
23. S. Yousefi et al., "Learning From Data: Recognizing Glaucomatous Defect Patterns and Detecting Progression From Visual Field Measurements," in IEEE Trans. on Biomedical Engg., vol. 61, no. 7, pp. 2112-2124, July 2014.
24. R. Panda, N. B. Puhan, A. Rao, D. Padhy and G. Panda, "Recurrent neural network based retinal nerve fiber layer defect detection in early glaucoma," 2017 IEEE 14th International Symposium on Biomedical Imaging (ISBI 2017), Melbourne, VIC, 2017, pp. 692-695.
25. M. E. Şahin and M. R. Bozkurt, "Retinal Nerve Fiber Layer detection at Optical Coherence Tomography image for the diagnosis of glaucoma,"2015 Medical Technologies National Conference, Bodrum, 2015, pp.1-3.
26. A. Gopalakrishnan, A. Almazroa, K. Raahemifar and V. Lakshminarayanan, "Optic disc segmentation using circular hough transform and curve fitting," 2015 2nd International Conference on Opto-Electronics and Applied Optics, Vancouver, BC, 2015, pp. 1-4.
27. T. Khalil, M. Usman Akram, S. Khalid and A. Jameel, "Improved automated detection of glaucoma from fundus image using hybrid structural and textural features," in IET Image Proc., vol. 11, no. 9, pp. 693-700, 9 2017.
28. N. Kavya and K. V. Padmaja, "Glaucoma detection using texture features extraction," 2017 51st Asilomar Conference on Signals, Systems, and Computers, Pacific Grove, CA, 2017, pp. 1471-1475.
29. S. Omid, J. Shanbehzadeh, Z. Ghassabi and S. S. Ostadzadeh, "Optic disc detection in high-resolution retinal fundus images by region growing," 2015 8th International Conference on Biomedical Engineering and Informatics (BMEI), Shenyang, 2015, pp. 101-105.
30. M. Lotankar, K. Noronha and J. Koti, "Detection of optic disc and cup from color retinal images for automated diagnosis of glaucoma," 2015 IEEE UP Section Conference on Electrical Computer and Electronics (UPCON), Allahabad, 2015, pp. 1-6.
31. G. Pavithra, A. Tugashetti, T. C. Manjunath and L. Dharmanna, "Investigation of primary glaucoma by CDR in fundus images," 2017 2nd IEEE International Conference on Recent Trends in Electronics, Information & Communication Technology (RTEICT), Bangalore, 2017, pp. 1841-1848.
32. W. Luangruangrong, K. Chinnasarn and A. Rodtook, "Polar Space Contour Detection for Automated Optic Cup Segmentation," 2018 10th International Conference on Knowledge and Smart Technology (KST), Chiang Mai, 2018, pp. 164-169.
33. P. Das, S. R. Nirmala and J. P. Medhi, "Detection of glaucoma using Neuroretinal Rim information," 2016 International Conference on Accessibility to Digital World (ICADW), Guwahati, 2016, pp. 181-186.
34. H. Alghmdi, Hongying Lilian Tang, M. Hansen, A. O'Shea, L. Al Turk and T. Peto, "Measurement of optical cup-to-disc ratio in fundus images for glaucoma screening," 2015 International Workshop on Computational Intelligence for Multimedia Understanding (IWCIM), Prague, 2015, pp. 1-5.
35. M. Aloudat and M. Faezipour, "Determination for Glaucoma disease based on red area percentage," 2016 IEEE Long Island Systems, Applications and Technology Conference (LISAT), Farmingdale, NY, 2016, pp. 1-5.
36. M. Roslin and S. Sumathi, "Glaucoma screening by the detection of blood vessels and optic cup to disc ratio," 2016 International Conference on Comm. and Signal Processing, Melmaruvathur, 2016, pp. 2210-2215.
37. S. M. Nikam and C. Y. Patil, "Glaucoma detection from fundus images using MATLAB GUI," 2017 3rd International Conference on Advances in Comp. Comm. & Automation (ICACCA) (Fall), Dehradun, 2017, pp. 1-4.
38. H. Ahmad, A. Yamin, A. Shakeel, S. O. Gillani and U. Ansari, "Detection of glaucoma using retinal fundus images," 2014 International Conference on Robotics and Emerging Allied Technologies in Engineering (iCREATE), Islamabad, 2014, pp. 321-324.
39. E. Pinos-Velez, M. Flores-Rivera, W. Ipanque-Alama, D. Herrera-Alvarez, C. Chacon and L. Serpa-Andrade, "Implementation of support tools for the presumptive diagnosis of Glaucoma through identification and processing of medical images of the human eye," 2018 IEEE International Systems Engineering Symposium (ISSE), Rome, 2018, pp. 1-5.
40. Atheesan S. and Yashothara S., "Automatic glaucoma detection by using funduscopic images," 2016 International Conference on Wireless Communications, Signal Processing and Networking (WiSPNET), Chennai, 2016, pp. 813-817.
41. J. K. Virk, M. Singh and M. Singh, "Cup-to-disk ratio (CDR) determination for glaucoma screening," 2015 1st International Conference on Next Generation Computing Technologies, Dehradun, 2015, pp. 504-507.
42. D. D. Patil, R. R. Manza, G. C. Bedke and D. D. Rathod, "Development of primary glaucoma classification technique using optic cup & disc ratio," 2015 International Conference on Pervasive Computing (ICPC), Pune, 2015, pp. 1-5.
43. D. E. Kusumandari, ArisMunandar and G. G. Redhyka, "The comparison of GVF Snake Active Contour method and Ellipse Fit in optic disc detection for glaucoma diagnosis," 2015 International Conference on Automation, Cognitive Science, Optics, Micro Electro-Mechanical System, and Information Technology (ICACOMIT), Bandung, 2015, pp. 123-126.
44. A. M. Jose and A. A. Balakrishnan, "A novel method for glaucoma detection using optic disc and cup segmentation in digital retinal fundus images," 2015 International Conference on Circuits, Power and Computing Technologies [ICCPCT-2015], Nagercoil, 2015, pp. 1-5.
45. E. Deepika and S. Maheswari, "Earlier glaucoma detection using blood vessel segmentation and classification," 2018 2nd International Conference on Inventive Systems and Control (ICISC), Coimbatore, 2018, pp. 484-490.
46. M. K. Dutta, A. K. Mourya, A. Singh, M. Parthasarathi, R. Burget and K. Riha, "Glaucoma detection by segmenting the super pixels from fundus colour retinal images," 2014 International Conf. on Medical Imaging, m-Health and Emerging Comm. Systems, Greater Noida, 2014, pp. 86-90.
47. K. Choudhary and S. Wadhwa, "Glaucoma Detection Using Cross Validation Algorithm," 2014 Fourth International Conference on Advanced Computing & Communication Technologies, Rohtak, 2014, pp. 478-482.
48. L. Xiong, H. Li and Y. Zheng, "Automatic detection of glaucoma in retinal images," 2014 9th IEEE Conference on Industrial Electronics and Applications, Hangzhou, 2014, pp. 1016-1019.
49. Harshvardhan G, Venkateswaran N and Padmapriya N, "Assessment of Glaucoma with ocular thermal images using GLCM techniques and Logistic Regression classifier," 2016 International Conference on Wireless Communications, Signal Processing and Networking (WiSPNET), Chennai, 2016, pp. 1534-1537.
50. S. Pathan, P. Kumar and R. M. Pai, "The Role of Color and Texture Features in Glaucoma Detection," 2018 International Conference on Advances in Computing, Communications and Informatics (ICACCI), Bangalore, 2018, pp. 526-530.
51. S. Simonthomas, N. Thulasi and P. Asharaf, "Automated diagnosis of glaucoma using Haralick texture features," International Conference on Information Communication and Embedded Systems (ICICES2014), Chennai, 2014, pp. 1-6.

52. Fu, Huazhu & Cheng, Jun & Xu, Yanwu & Zhang, Changqing & Wing Kee Wong, Damon & Liu, Jiang & Cao, Xiaochun. (2018). Disc-Aware Ensemble Network for Glaucoma Screening From Fundus Image. IEEE Transactions on Medical Imaging. PP. 1-1. 10.1109/TMI.2018.2837012.
53. A. Pal, M. R. Moorthy and A. Shahina, "G-Eyenet: A Convolutional Autoencoding Classifier Framework for the Detection of Glaucoma from Retinal Fundus Images," 2018 25th IEEE International Conference on Image Processing (ICIP), Athens, 2018, pp. 2775-2779.
54. X. Chen, Y. Xu, D. W. Kee Wong, T. Y. Wong and J. Liu, "Glaucoma detection based on deep convolutional neural network," 2015 37th Annual International Conference of the IEEE Engineering in Medicine and Biology Society (EMBC), Milan, 2015, pp. 715-718.
55. F. Calimeri, A. Marzullo, C. Stamile and G. Terracina, "Optic Disc Detection Using Fine Tuned Convolutional Neural Networks," 2016 12th International Conference on Signal-Image Technology & Internet-Based Systems (SITIS), Naples, 2016, pp. 69-75.
56. J. Kim, S. Candemir, E. Y. Chew and G. R. Thoma, "Region of Interest Detection in Fundus Images Using Deep Learning and Blood Vessel Information," 2018 IEEE 31st International Symposium on Computer-Based Medical Systems (CBMS), Karlstad, 2018, pp. 357-362.
57. A. John, A. Sharma, H. Singh and V. Rehani, "Fuzzy based decision making for detection of Glaucoma," 2017 8th International Conference on Computing, Communication and Networking Technologies (ICCCNT), Delhi, 2017, pp. 1-6.
58. C. Gisler, A. Ridi, M. Fauquex, D. Genoud and J. Hennebert, "Towards glaucoma detection using intraocular pressure monitoring," 2014 6th International Conference of Soft Computing and Pattern Recognition (SoCPaR), Tunis, 2014, pp. 255-260.
59. Gayatri. R., P. V. Rao and A. S., "Automated glaucoma detection system based on wavelet energy features and ANN," 2014 International Conference on Advances in Computing, Communications and Informatics (ICACCI), New Delhi, 2014, pp. 2808-2812.
60. J. Ayub et al., "Glaucoma detection through optic disc and cup segmentation using K-mean clustering," 2016 International Conference on Computing, Electronic and Electrical Engg., Quetta, 2016, pp. 143-147.
61. Y. Hatanaka et al., "Improved automated optic cup segmentation based on detection of blood vessel bends in retinal fundus images," 2014 36th Annual International Conference of the IEEE Engineering in Medicine and Biology Society, Chicago, IL, 2014, pp. 126-129.
62. A. Chakravarty and J. Sivaswamy, "Glaucoma classification with a fusion of segmentation and image-based features," 2016 IEEE 13th International Symposium on Biomedical Imaging (ISBI), Prague, 2016, pp. 689-692.
63. A. Ramzan, M. Usman Akram, A. Shaukat, S. Gul Khawaja, U. Ullah Yasin and W. Haider Butt, "Automated glaucoma detection using retinal layers segmentation and optic cup-to-disc ratio in optical coherence tomography images," in IET Image Processing, vol. 13, no. 3, pp. 409-420, 28 2 2019.
64. A. Agarwal, A. Issac, A. Singh and M. K. Dutta, "Automatic imaging method for optic disc segmentation using morphological techniques and active contour fitting," 2016 Ninth International Conference on Contemporary Computing (IC3), Noida, 2016, pp. 1-5.
65. S. A. Tuncer, T. Selçuk, M. Parlak and A. Alkan, "Hybrid approach optic disc segmentation for retinal images," 2017 International Artificial Intelligence and Data Processing Symposium, Malatya, 2017, pp. 1-5.
66. A. Agarwal, S. Gulia, S. Chaudhary, M. K. Dutta, C. M. Travieso and J. B. Alonso-Hernández, "A novel approach to detect glaucoma in retinal fundus images using cup-disk and rim-disk ratio," 2015 4th International Work Conference on Bioinspired Intelligence (IWOBI), San Sebastian, 2015, pp. 139-144.